A potential histone-chaperone activity for the MIER1 histone deacetylase complex

Siyu Wang[1], Louise Fairall[1], Trong Khoa Pham[2,3], Timothy J. Ragan[1], Dipti Vashi[1], Mark O. Collins [2,3], Cyril Dominguez [1] and John W.R. Schwabe [1,*]

[1]Institute for Structural and Chemical Biology & Department of Molecular and Cell Biology, University of Leicester, Leicester LE1 7RH, UK, [2]School of Biosciences, University of Sheffield, Sheffield S10 2TN, UK and [3]biOMICS facility, Mass Spectrometry Centre, University of Sheffield, Sheffield S10 2TN, UK

ABSTRACT

Histone deacetylases 1 and 2 (HDAC1/2) serve as the catalytic subunit of six distinct families of nuclear complexes. These complexes repress gene transcription through removing acetyl groups from lysine residues in histone tails. In addition to the deacetylase subunit, these complexes typically contain transcription factor and/or chromatin binding activities. The MIER:HDAC complex has hitherto been poorly characterized. Here, we show that MIER1 unexpectedly co-purifies with an H2A:H2B histone dimer. We show that MIER1 is also able to bind a complete histone octamer. Intriguingly, we found that a larger MIER1:HDAC1:BAHD1:C1QBP complex additionally co-purifies with an intact nucleosome on which H3K27 is either di- or tri-methylated. Together this suggests that the MIER1 complex acts downstream of PRC2 to expand regions of repressed chromatin and could potentially deposit histone octamer onto nucleosome-depleted regions of DNA.

INTRODUCTION

The histone deacetylase enzymes, HDACs 1 and 2 act as epigenetic 'erasers' removing acetyl groups from histone tails (1). This results in the loss of binding sites for regulatory 'reader' proteins and causes chromatin compaction by restoring the positive charge on histone tails. HDACs 1 and 2 are highly homologous enzymes that are assembled into six distinct multiprotein complexes: NuRD, CoREST, Sin3A/B, MiDAC, RERE and MIER (2–7). There appears to be little or no redundancy between these complexes since mice lacking unique components typically die during embryogenesis (5,8–10). Apart from the HDAC enzyme, the complexes differ in subunit composition, but often contain chromatin and/or transcription factor interaction activities. The MIER complex has to date received relatively little at-

tention, but is likely to have an important regulatory function since it is present from nematodes to man.

The MIER complex is named after the MIER co-repressor scaffold proteins that directly recruit HDAC1/2 through a canonical ELM2-SANT domain (11). There are three paralogous genes mier1, 2 and 3. MIER1, also known as Mesoderm Induction Early Response protein 1, was first identified as a fibroblast growth factor regulated gene in Xenopus laevis (4,12). The central ELM2-SANT domain of MIER1, 2 and 3 is highly conserved; the amino-terminal region is moderately conserved (Supplementary Figure S1a) and the carboxy-terminal region is poorly conserved. The MIER proteins are predominantly located in the nucleus (12).

Several studies have shown that the BAH domain-containing protein, BAHD1, interacts with the MIER1:HDAC1 complex (13,14). BAH domains are found in many chromatin-associated proteins including several proteins involved in transcriptional repression such as SIR3, MTA1, RERE, BAHCC1 and BAHD1 (15,16). BAH domains have been shown to mediate interaction both with intact nucleosomes and with specific histone marks such as H4K20me2 and H3K27me3 (17–20). Both BAHCC1 and BAHD1 recognise H3K27me3 suggesting that they are 'reader' domains acting downstream of the PRC2 complex (10,21). It is unclear, however, whether these BAH domains simply recognise the H3K27me3 histone mark, or whether they can bind to intact nucleosomes in an analogous fashion to the BAH-containing proteins ORC1 and SIR3 (17,20).

Here, we report a biochemical and functional study of the MIER1:HDAC1 and MIER1:HDAC1:BAHD1 complexes. We find that the MIER1 amino-terminal domain mediates interaction with histones H2A and H2B and is able to bind to an intact histone octamer. The MIER1:HDAC1:BAHD1 complex co-purifies with the multi-functional protein C1QBP and with an intact nucleosome specifically bearing H3K27me2/3 marks. The finding that a histone deacetylase complex binds histone octamer

*To whom correspondence should be addressed. Tel: +44 116 2297030; Email: john.schwabe@leicester.ac.uk

and may therefore potentially act to recruit or deposit histones is unexpected, but makes sense in terms of increasing nucleosome density as part of a transcriptional repression activity.

MATERIALS AND METHODS

Mammalian protein expression and purification

MIER1 constructs were cloned into pcDNA3.0 expression vectors containing an amino-terminal 10xHis-3xFLAG tag followed by a TEV protease cleavage site. Full length HDAC1(aa:1–482) and BAHD1(aa:525–780) were cloned without affinity tags into the same vectors. Constructs were co-transfected in HEK293F suspension grown cells (Invitrogen) using polyethylenimine (PEI; Sigma) as a transfection reagent and harvested after 48 h. Cells were lysed in buffer containing 50 mM Tris/HCl pH 7.5, 50 mM potassium acetate, 5% v/v glycerol, 0.4% v/v Triton X-100 and Complete EDTA-free protease inhibitor (Roche). The lysate was clarified by centrifugation and applied to Anti-FLAG M2 affinity resin (Sigma Aldrich) for 30 min and washed three times with 50 mM Tris/HCl pH 7.5, 50 mM potassium acetate and 5% v/v glycerol and three times more with 50 mM Tris/HCl pH 7.5, 50 mM potassium acetate and 0.5 mM TCEP before being cleaved by TEV protease overnight. The protein complexes were purified further by gel filtration using a Superdex S200 column (Cytiva) with buffer containing 25 mM Tris/HCl pH 7.5, 50 mM potassium acetate and 0.5 mM TCEP.

E. coli protein expression and purification

Truncated MIER1 was cloned into pGEX expression vectors containing an amino-terminal GST-tag followed by a TEV protease cleavage site and the recombinant protein was over expressed in *Escherichia coli* strain Rosetta (DE3). Bacterial cultures were grown at 37°C to an optical density of ~0.6, the temperature of the culture was reduced to 20°C and protein expression was induced by addition of isopropyl-β-ᴅ-thiogalactopyranoside (IPTG) to a final concentration of 40 μM. The cells were harvested after the cultures were grown for a further 16 h. The cells were lysed in lysis buffer containing phosphate buffered saline (PBS), 1% v/v Triton X-100, 1 mM Dithiothreitol (DTT) and Complete EDTA-free protease inhibitor (Roche). The soluble fraction was then incubated with Glutathionine Sepharose (Cytiva) resin for 1 hour at 4°C with gentle agitation. The protein-bound resin was then washed three times with wash buffer (1 × PBS, 1% v/v Triton X-100, 1 mM DTT) and then three times more with cleavage buffer (1 × PBS, 1 mM DTT). The GST-tag was removed by incubation with TEV protease overnight at 4°C. The TEV-cleaved protein was concentrated to around 500 μl using a 4 ml Amicon® Ultra centrifugal filter concentrator (Merck Millipore) with a membrane molecular weight cut-off of 10 kDa. The concentrated protein was filtered through a 0.22 μm centrifugal filter (Merck Millipore) prior to loading onto the gel filtration column. The protein sample was purified on a Superdex S200 (10/300) GL column (Cytiva) with buffer containing 25 mM Tris/Cl pH 7.5, 50 mM potassium acetate and 0.5 mM TCEP. 500 μl fractions were collected and 10 μl

of the fractions was taken for analysis on NuPAGE 4–12% Bis-Tris gels (Invitrogen). Fractions containing the purified protein were concentrated using a 0.5 ml Amicon Ultra centrifugal filter (Merck Millipore) with a membrane molecular weight cut-off of 10 kDa.

Histone purification

Human histones cloned into pET3a (plasmids were a gift from Martin Browne and Andrew Flaus NUI Galway) were expressed separately in Rosetta2 (DE3) pLysS (Novagen). Cell pellets were resuspended in 30 ml histone wash buffer which contained 50 mM Tris/Cl pH 7.5, 100 mM NaCl, 5 mM DTT and Complete EDTA-free protease inhibitor (Roche). After sonication, the insoluble fractions were pelleted by spinning at 4°C at 30 000 g for 15 min and washed twice with wash buffer containing 50 mM Tris/Cl pH 7.5, 100 mM NaCl, 5 mM DTT, 1% Triton X-100 and Complete EDTA-free protease inhibitor (Roche) and three times with wash buffer without Triton X-100. To resuspend the inclusion bodies 0.5 ml of DMSO was then added and incubated at room temperature for 30 min on a roller then 5 ml unfolding buffer containing 7 M guanidine HCl, 20 mM Tris/Cl pH 7.5 and 10 mM DTT was added, and the incubation continued for an additional 1 h.

After the pellet was fully dissolved, 70 ml 7 M urea, 50 mM Tris/Cl pH 7.5 and 1 mM EDTA was added and the sample was centrifuged at 35 000 × g for 20 min. The histone solution was then filtered through a 0.22 μm filter prior to loading onto a HiTrap Q HP. The flow through was then loaded onto a HiTrap SP HP. The histones were eluted with a gradient to 2 M NaCl. Fractions containing histone were then dialysed with three changes into buffer containing 0.1% acetic acid and 5 mM DTT. They were then freeze dried in aliquots.

Histone octamer refolding and nucleosome reconstitution

Equimolar amounts of H2A, H2B, H3 and H4 were dissolved in unfolding buffer which contained 7 M guanidine, 20 mM Tris pH 7.5 and 10 mM DTT and mixed with a small excess of H2A and H2B. The histone mix was dialysed against high salt buffer (20 mM Tris pH 7.5, 2.0 M NaCl, 1 mM EDTA and 5 mM mercaptoethanol) and then purified by size exclusion chromatography using a Superdex S200 column.

For the nucleosome reconstitution, 157 bp of 601 DNA was amplified by PCR from a 601 DNA template ([22](#)). The histone octamer and 157 bp DNA were mixed in equimolar amounts in 15 mM HEPES pH 7.5, 2 M KCl, 5% glycerol, 0.1% Triton X-100, 0.5 mM TCEP and dialysed stepwise to 15 mM HEPES pH 7.5, 50 mM KCl, 5% glycerol, 0.1% Triton X-100, 0.5 mM TCEP.

Size exclusion chromatography with multi-angle light scattering (SEC-MALS)

Gel filtrated pure MIER1(aa:171–350):HDAC1 complex was reapplied to a Superdex S200 column and monitored with an Optilab T-rEX differential Refractive index detector connected to a DAWN HELEOS MALS detector

(Wyatt Technology). The mass of the complex was calculated using ASTRA software version 6.1.

Boc-lys(ac)-AMC HDAC assay

A fluorescent based HDAC assay was used to determine HDAC activity of the MIER1 complex with BOC-lys(Ac)-AMC (BaChem) as the substrate. For these experiments, 20 nM MIER1(aa:171–350):HDAC1 complex (alone or with 100 μM Ins(1,2,3,4,5,6)P$_6$ or 30 μM SAHA or 30 μM MS275) in 25 mM Tris/Cl, pH 7.5 and 50 mM NaCl were incubated in a shaking incubator at 37°C for 30 min before adding 100 μM substrate for a further 30 min. The assay was developed by the addition of developer solution (2 mM TSA, 10 mg/ml Trypsin, 50 mM Tris pH 7.5, 100 mM NaCl). Fluorescence was measured at 335/460 nm using a Victor X5 plate reader (Perkin Elmer). Data was analysed using GraphPad Prism 9.0.

Isothermal titration calorimetry (ITC)

The ITC experiment was performed using a VP-ITC instrument (MicroCal). H2A/H2B dimer (4.6 μM) was loaded in the sample cell and 170 μM of MIER1(aa:1–177) in the syringe. The titration experiment was performed at 25°C and consisted of 30 injections of 5 μl each with a 5 min interval between additions. The raw data were integrated, corrected for nonspecific heat, normalized for the molar concentration and analysed according to a 1:1 binding model.

NMR measurement

For NMR sample preparation, MIER1(aa:1–177) was uniformly labelled by overexpression in M9 minimum medium, containing ^{15}NH$_4$Cl as the sole nitrogen source. The expression and purification of labelled MIER1 was performed as described above. MIER1(aa:1–177) (200 μM) with 10% D$_2$O in a final volume of 330 μl of PBS buffer was placed in 3 mm NMR tubes (Norell). (^{15}N–^{1}H)-HSQC spectra were measured on a Bruker AVIII-600 MHz spectrometer equipped with a cryoprobe. Data were processed using Topspin (Bruker) and analysed with Sparky. H2A:H2B dimer was added to the labelled MIER1(aa:1–177) protein at the ratio of 1:1 and incubated for 30 min at 4°C. The MIER1(aa:1–177):H2A:H2B complex was then purified on a Superdex S200 column before collecting (^{15}N–^{1}H) HSQC NMR data.

Western blot

Western blotting was carried out using NuPAGE 4–12% Bis-Tris gels (Invitrogen) and a semi-dry transfer system with nitrocellulose membranes. Membranes were blocked for 1 h at room temperature using 5% skimmed milk TBS/T and incubated with the primary mouse antibody C1QBP (1:1000 H-9:sc-271200, Santa Cruz) diluted in blocking buffer overnight at 4°C. Secondary antibody goat anti-mouse 680RD (1:10 000, LI-COR), was incubated with membranes for 1 h at room temperature and detected using an Odyssey CLx digital imaging system (LI-COR).

GST-pull down experiment

GST-MIER1(aa:1–177) and GST tag alone were purified separately without eluting the proteins from the glutathione sepharose resin (Cytiva) in PBS, 1 mM TCEP and Complete EDTA-free protease inhibitor (Roche). Excess octamer and nucleosome were mixed either with the GST-tagged MIER1 or with the GST-tag alone and incubated for 30 min at 4°C. After washing 5 times with PBS, 0.5 mM TCEP, the samples were analysed on an 18% SDS-PAGE gel.

DNA extraction

50 U/μl micrococcal nuclease and 10 mM CaCl$_2$ was added to the purified MIER1(aa:171–512):HDAC1:BAHD1(aa:525–780):C1QBP complex. This was incubated for 30 min at 37°C and EDTA to 10 mM was added to stop the reaction. 10 μl of proteinase K and 1% SDS were added and incubated for 30 min at 37°C. This was then adjusted to 1 M NaCl and phenol:chloroform:isoamyl alcohol extracted. The DNA was ethanol precipitated, analysed on a 1× TBE, 1% agarose gel and visualised with ethidium bromide.

Fluorescence polarisation assay

Fluorescence polarisation experiments were performed using fluorescently 5-FAM (5-carboxyfluorescein) labelled histone peptides (Cambridge Research Biochemicals).

- H3 1–19ARTKQTARKSTGGKAPRKQ-ed-[4-Abu]-[5-FAM]
- H3 1–19 K4me3ART-[Lys(Me3)]-QTARKSTGGKAPRKQ-ed-[4-Abu]-[5-FAM]
- H3 1–19 K9me3ARTKQTAR-[Lys(Me3)]-STGGKAPRKQ-ed-[4-Abu]-[5-FAM]
- H3 16–35PRKQLATKAARKSAPATGG-ed-[4-Abu]-[5-FAM]
- H3 16–35 R26me2aPRKQLATKAA-[ADMA]-KSAPATGG-ed-[4-Abu]-[5-FAM]
- H3 16–35 K27me3PRKQLATKAAR-[Lys(Me3)]-SAPATGG-ed-[4-Abu]-[5-FAM]

(ADMA: asymmetric dimethyl arginine; Abu: aminobutyric acid; ed: ethylene diamine linker)

The assays were performed in black 384-well assay plates with a non-binding surface (Corning Life Sciences). Multiple titrations were performed using a fixed concentration of 5 nM histone peptide with increasing concentrations of *E. coli* expressed BAHD1(aa:588–780) (0–142 μM) in a final volume of 25 μl in 25 mM Tris/Cl, pH 7.5 and 50 mM NaCl. The plate was incubated in the shaking incubator for 15 min at 37°C, then centrifuged at 61 g for 10 s and the data were acquired in a Victor X 5 plate reader (Perkin Elmer) with an excitation wavelength of 480 nm and an emission wavelength of 535 nm. The subsequent data were analysed with GraphPad Prism 9.0. K_d values were calculated by nonlinear curve fitting with a one-site binding model.

Mass spectrometry analysis

Propionylation of histones and in-gel digestion. Gel bands were derivatised according to (23,24) with some modifica-

tions. Briefly, 50 μl of 50 mM ammonium bicarbonate was added to the gel pieces and incubated with 16.6 μl of propionylation reagent (1:3 v/v propionic anhydride in acetonitrile) for 15 min at 37°C with agitation in a thermomixer at 900 rpm (Eppendorf, UK). The supernatant was then removed and the derivatisation process was repeated. After discarding the supernatant, the gel was de-stained, and proteins were reduced with 10 mM dithiothreitol for 1 h at 55°C and then alkylated with 55 mM iodoacetamide for 20 min at room temperature in the dark. Protein in the gel was digested with 100 μl of trypsin (0.02 μg/μl) at 37°C overnight. Peptides were then extracted twice with 100 μl of 3.5% formic acid in 30% ACN then followed by 5% formic acid in 50% ACN. Eluted peptides were dried in a vacuum concentrator and stored at −20°C until MS analysis.

MS and data analyses. Peptides were resuspended in 0.5% formic acid and analysed using an Orbitrap Elite (Thermo Fisher) hybrid mass spectrometer equipped with a nanospray source, coupled to an Ultimate RSLCnano LC System (Dionex). Peptides were desalted online using a nano trap column, 75 μm I.D. × 20 mm (Thermo Fisher) and then separated using a 120-min gradient from 5 to 35% buffer B (0.5% formic acid in 80% acetonitrile) on an EASY-Spray column, 50 cm × 50 μm ID, PepMap C18, 2 μm particles, 100 Å pore size (Thermo Fisher). The Orbitrap Elite was operated with a cycle of one MS (in the Orbitrap) acquired at a resolution of 120 000 at m/z 400, with the top 20 most abundant multiply charged (2 + and higher) ions in a given chromatographic window subjected to MS/MS fragmentation in the linear ion trap. An FTMS target value of 1e6 and an ion trap MSn target value of 1e4 were used with the lock mass (445.120025) enabled. Maximum FTMS scan accumulation time of 200 ms and maximum ion trap MSn scan accumulation time of 50 ms were used. Dynamic exclusion was enabled with a repeat duration of 45 s with an exclusion list of 500 and an exclusion duration of 30 s. Raw mass spectrometry data were analysed with MaxQuant version 1.6.10.43 (25). Data were searched against a human UniProt reference proteome (downloaded June 2022) using the following search parameters for standard protein identification: enzyme set to Trypsin/P (2 mis-cleavages), methionine oxidation and N-terminal protein acetylation as variable modifications, cysteine carbamidomethylation as a fixed modification. For histone PTM analysis the following settings were used: enzyme set to Trypsin/P with up to 5 missed cleavages, methionine oxidation, lysine propionylation, lysine acetylation, lysine mono, di and trimethylation were set as variable modifications, cysteine carbamidomethylation as a fixed modification. A protein FDR of 0.01 and a peptide FDR of 0.01 were used for identification level cut-offs based on a decoy database searching strategy. MaxQuant calculated intensities of peptides containing PTMs (lysine acetylation, lysine mono, di and trimethylation) were normalised (divided) to unmodified versions of corresponding peptides. Biological triplicates were performed for each group, mean and standard deviation (SD) were then determined using GraphPad Prism 9.0. Raw MS data and searched results from MaxQuant are available from PRIDE (https://www.ebi.ac.uk/pride/) with identifier PXD040685.

RESULTS

MIER1 binds to HDAC1/2 through the ELM2-SANT domain

We have previously shown that the ELM2-SANT domains from MTA1, MIDEAS and RCoR1 mediate interaction of the NuRD, MiDAC and CoREST complexes with HDACs 1 and 2 (5–7). To confirm that the homologous ELM2-SANT domain from MIER1 is also capable of binding HDAC1/2 we co-expressed FLAG-tagged MIER1(aa:171–350) with full-length HDAC1 in HEK293F cells (Figure 1). Affinity purification on anti-FLAG resin, followed by size exclusion chromatography confirmed the expected interaction (Figure 1B). The elution profile is consistent with a monomeric 1:1 complex. This was confirmed using size exclusion chromatography coupled with multi-angle light scattering (SEC-MALS). The complex molecular weight was determined to be 73.6 ± 1.5 kDa (Figure 1C), which is consistent with a monomeric complex (HDAC1 55 kDa + MIER1(aa:171–350) 21 kDa) and contrasts with the dimeric MTA1 and tetrameric MIDEAS complexes (5,7). HDAC assays confirmed that the complex is active; can be further activated by inositol-hexakis-phosphate and is inhibited by hydroxamic and benzamide-based inhibitors (Figure 1D). We used Alphafold2 multimer (26) to predict the structure of the MIER1-ELM2-SANT domain bound to HDAC1 (Figure 1E). The region of the ELM2 domain that mediates dimerization in MTA1 is clearly unable to support dimerization in MIER1. Helix 2 is absent in MIER1 and the non-polar residues located at the MTA1 dimer interface are mostly replaced with basic residues in MIER1 (Figure 1F).

The amino terminal region of MIER1 co-purifies with endogenous H2A:H2B histone dimers

To characterise the native complex, we co-expressed FLAG-tagged full-length MIER1 in HEK293F mammalian cells, together with full-length HDAC1. Following purification, we observed the expected 1:1 interaction with HDAC1 (Figure 2A). Unexpectedly however, in addition to the bands for MIER1 and HDAC1, we observed two low molecular-weight proteins that co-purify with the complex through both the affinity and size exclusion purifications. Mass-spectrometry (MS) analysis of these bands identified these proteins to be endogenous histones H2A and H2B (Figure 2A).

This unexpected interaction with histones H2A and H2B was not observed with the isolated ELM2-SANT domain (Figure 1B) suggesting that either the amino-terminal or carboxy-terminal regions mediate this interaction. To identify the interaction region, we expressed FLAG-tagged MIER1(aa:1–177) and FLAG-tagged MIER1(aa:346–512). The H2A:H2B dimer co-purified with the amino-terminal construct and not with the carboxy-terminal construct. Furthermore, the coomassie staining is consistent with a stoichiometric 1:1:1 complex (Figure 2B).

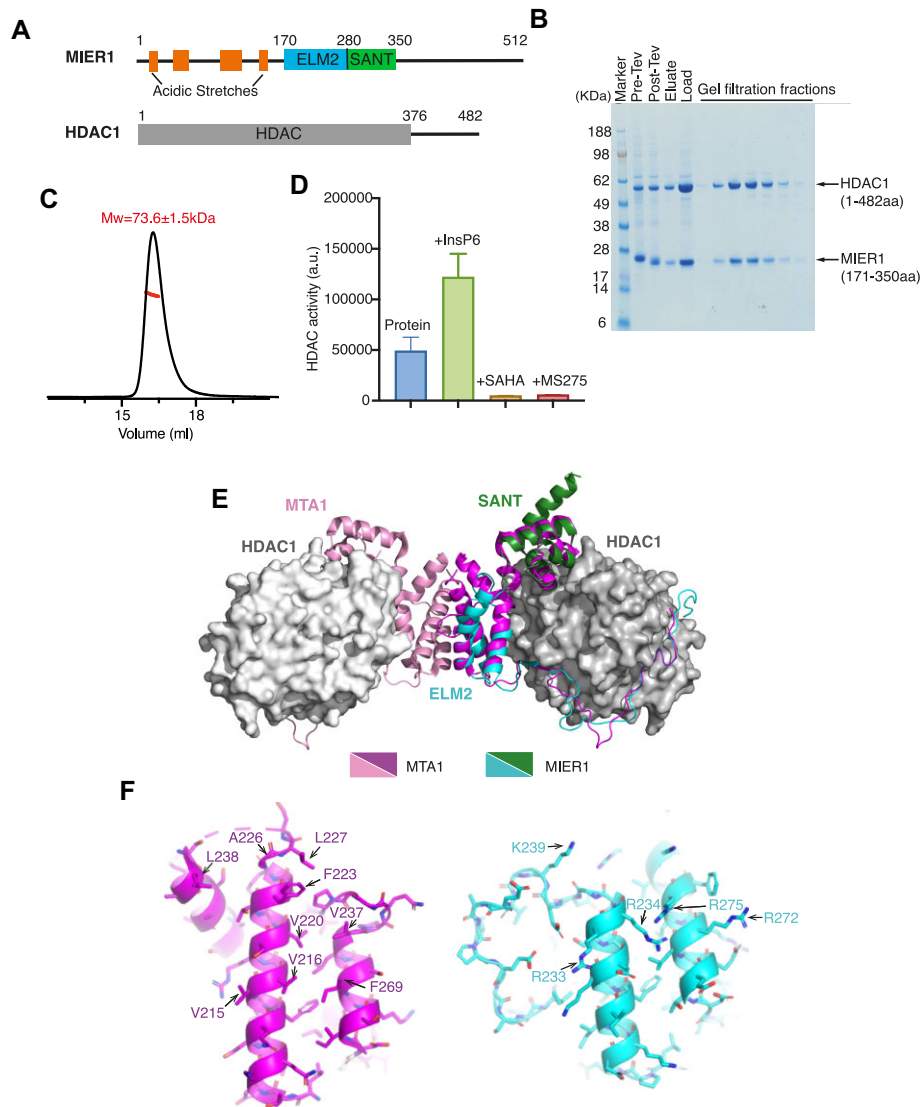MIER1 has two paralogues MIER2 and MIER3. Whilst the ELM2-SANT domain is highly conserved

Figure 1. The ELM2-SANT domain of MIER1 co-purifies with HDAC1 and forms a stable, stoichiometric, enzymatically active complex. (**A**) Schematic of the domain structure of full-length MIER1 and HDAC1. (**B**) Purification of the FLAG-tagged MIER1 ELM2-SANT (aa:171–350):HDAC1 complex using Anti-FLAG resin followed by a Superdex S200 size exclusion column shown on a SDS-PAGE gel. 'Pre-TEV' indicates the protein bound to resin before eluting with TEV protease. 'Post-TEV' indicates the resin with supernatant following digestion with TEV protease. 'Elute' indicates the supernatant after TEV digestion. 'Load' indcates the concentrated sample before gel filtration. (**C**) Determination of the stoichiometry/molecular weight of the MIER1 ELM2-SANT (aa:171–350):HDAC1 complex using SEC-MALS. The theoretical molecular weight is 75 kDa and the measured molecular weight for 1:1 stoichiometry is 73.6 ± 1.5 kDa. (**D**) Deacetylase activity of the MIER1 ELM2-SANT (aa:171–350):HDAC1 complex alone and in the presence of 100 μM Ins(1,2,3,4,5,6)P6 (InsP6), 30 μM SAHA and 30 μM MS275. The background of the assay with no complex has been subtracted. Error bars indicate the SEM ($n = 3$). (**E**) Alphafold2 multimer prediction for the ELM2-SANT domain of MIER1(aa:171–350) (cyan-forest green) with HDAC1(grey) complex compared with the crystal structure of the MTA1(aa:162–354) (pink/magenta):HDAC1(grey) complex (4BKX). (**F**) Dimerisation interface of ELM2 domain from MTA1(magenta) compared with ELM2 domain of MIER1(cyan).

(63% identity), the amino-terminal region is less well conserved (Figure 2E – a cross-species alignment is shown in Supplementary Figure S1a). To determine whether histone binding is a conserved feature of the MIER proteins, we expressed both full-length and the amino-terminal domain of MIER3 in HEK293F cells. Both constructs of MIER3 co-purified with histones H2A:H2B (Figure 2C) suggesting that histone binding is a common and important property of this family of HDAC co-repressor proteins. Interestingly, in several experiments, we found that histones H3 and H4

also co-purify with the MIER proteins (Figure 2D). Since this interaction does not survive gel filtration, we believe that this is a relatively weak interaction (*in vitro*) mediated by interaction between H2A:H2B heterodimer with H3:H4. In contrast, we infer from the fact that the H2A:H2B heterodimer co-purifies with MIER1 over both affinity and size-exclusion columns that the interaction must be relatively strong, or at least the off-rate is slow. Using isothermal calorimetry we measured a dissociation constant of between 227 and 383 nM (Figure 3A).
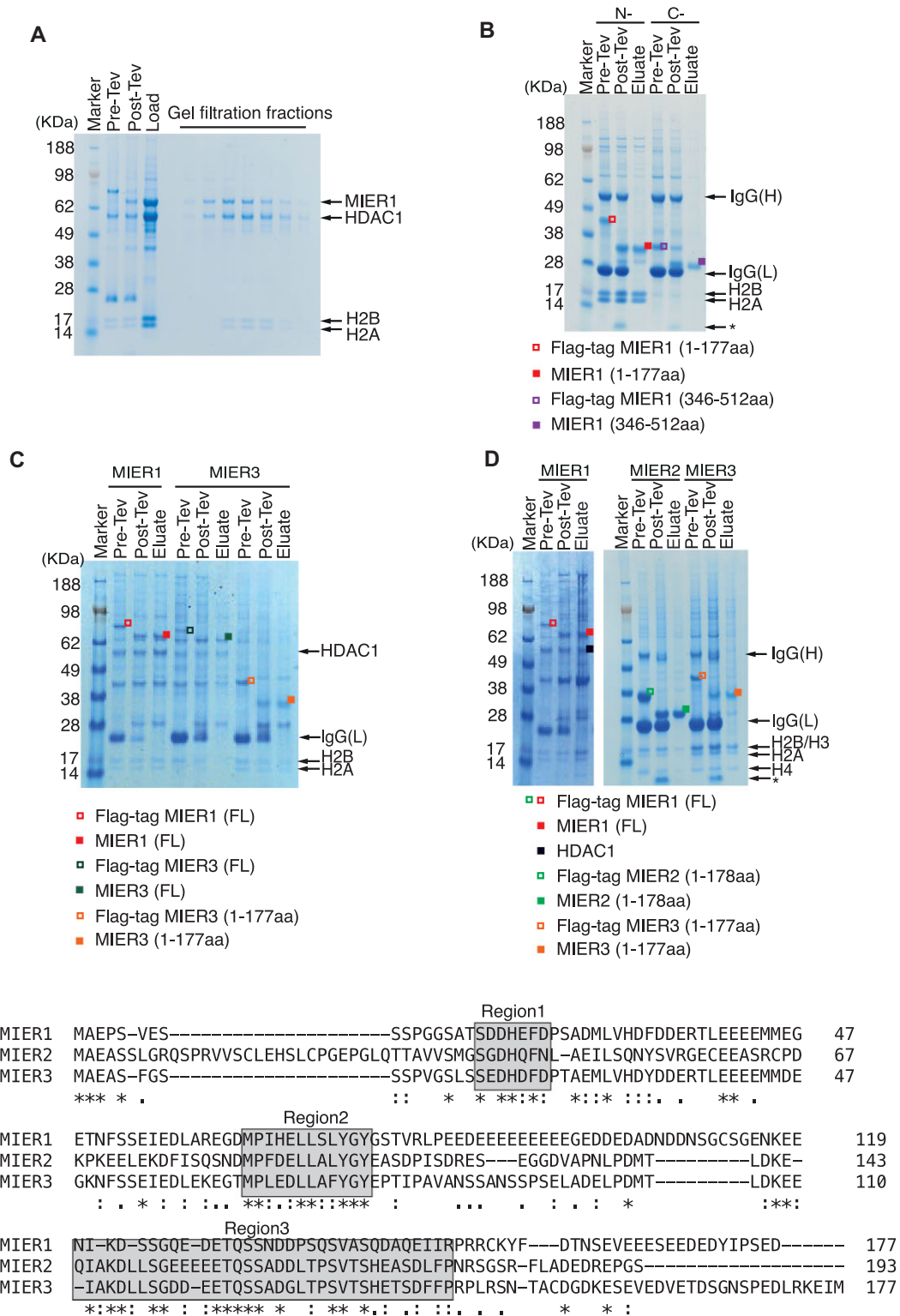
Figure 2. Interaction of MIER 1, 2 and 3 with a histone H2A:H2B dimer. (**A**) Full length FLAG tagged MIER1(aa:1–512):HDAC1 complex co-purifies with endogenous H2A and H2B. SDS-PAGE showing the purification with Anti-FLAG resin and the fractions from the Superdex S200 size exclusion column. (**B**) The amino-terminus of MIER1(aa:1–177) (LHS red symbols) interacts with a histone H2A:H2B dimer. The C-terminus of MIER1(aa:346–512) (RHS purple symbols) shows no interaction. * indicates cleaved tag. (**C**) Full length FLAG tagged MIER1(aa:1–512) (red symbols) purifies with endogenous HDAC, H2A and H2B. Full length FLAG tagged MIER3(aa:1–553) (green symbols) and amino-terminus of MIER3(aa:1–177) (orange symbols) co-purify with endogenous H2A:H2B. (**D**) Full length FLAG tagged MIER1(aa:1–512) (red symbols) purifies with endogenous HDAC1(black symbol), H2A and H2B. MIER2(aa:1–178) (green symbols) and MIER3(aa:1–177) (orange symbols) co-purify with endogenous H2A:H2B. * indicates cleaved tag. (**E**) Sequence alignment of the amino termini of MIER1, MIER2 and MIER3. Identical and conserved residues are highlighted in grey boxes. Identical residues are labelled with stars, strong similarity is labelled with two dots and a single dot indicates weak similarity.
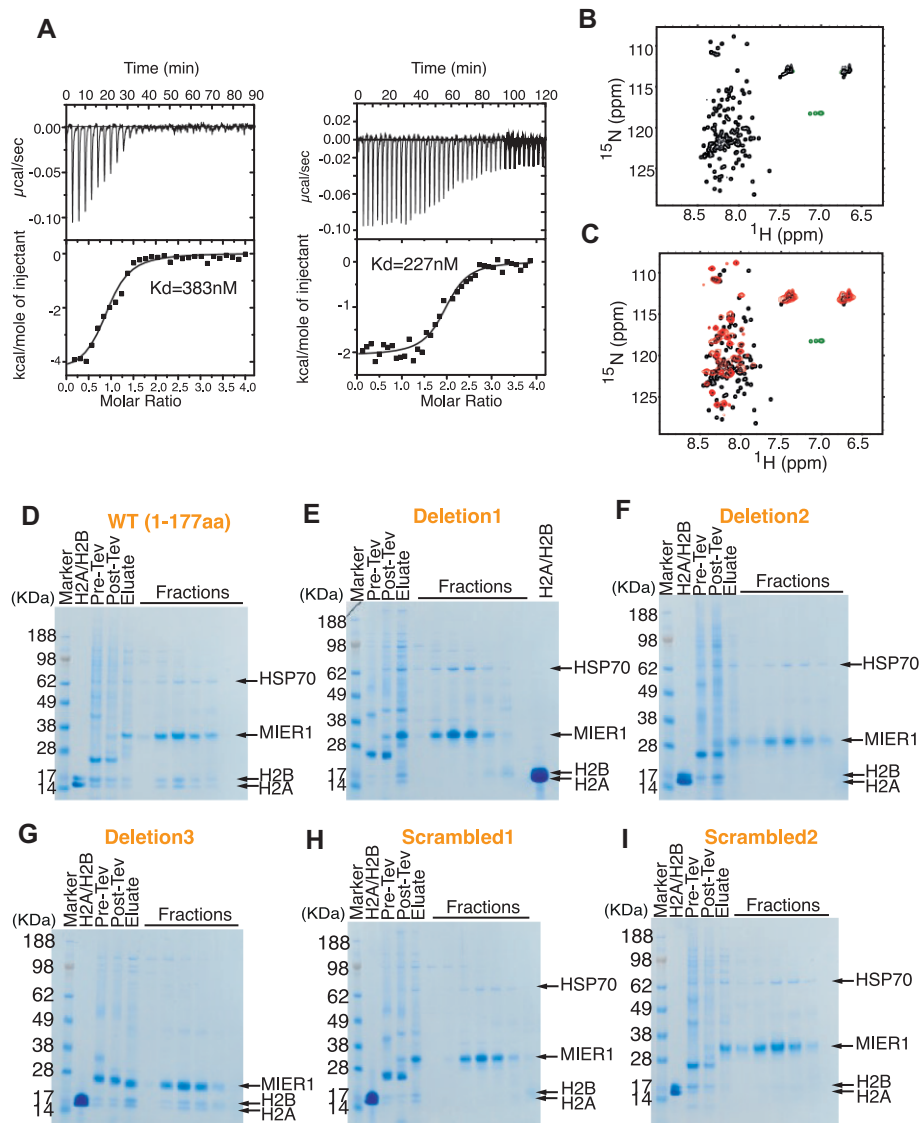
Figure 3. Characterisation of the interaction between amino-terminus of MIER1(aa:1–177) and endogenous H2A:H2B dimer. (**A**) Isothermal titration calorimetry of MIER1(aa:1–177) binding to histones H2A:H2B Raw calorimetric outputs are shown on top and binding isotherms describing formation of the MIER1(aa:1–177):H2A:H2B complex are shown at the bottom. (**B**) (1H-15N) HSQC experiment of the labelled MIER1(aa:1–177) protein in 1x PBS pH 7.4 and 0.5 mM TCEP. (**C**) HSQC results of MIER1(aa:1–177) with the addition of histone H2A and H2B (red) at ratio 1:1 compared with free MIER1(black). (**D–I**) The Flag-tagged wild type MIER1(aa:1–177) and scrambled/deletion regions of MIER1 were expressed in the HEK 293F cells, purified with Anti-FLAG resin followed by a Superdex S200 column. D1, D2, D3, S1 or S2 are the deleted or scrambled regions 1, 2 or 3 of MIER1 and are shown in Supplementary Figure S1. The lanes marked H2A/H2B contains *E. coli* expressed H2A:H2B complex purified on a Resource S column followed by a Superdex S200 column.

Further confirmation of interaction was obtained using NMR spectroscopy. ^{15}N-labelled MIER1(aa:1–177) was expressed in *E. coli* and was mixed in a 1:1 ratio with unlabelled H2A:H2B dimer (expressed separately). The limited ^{1}H chemical shift distribution of MIER1 in an HSQC spectrum is typical of an intrinsically disordered protein (Figure 3B). Following addition of the H2A:H2B dimer, the HSQC spectrum clearly shows both chemical shift perturbations and a general broadening consistent with MIER1 binding the folded histone dimer (Figure 3C). Approximately half the amino acids in MIER1(aa:1–177) appear to be involved in the interaction.

Histone binding activity maps to two regions of conservation in the amino-termini of MIER proteins

To investigate which regions of the amino-terminus of MIER1 mediated the interaction with H2A:H2B, we hypothesised that regions conserved between MIER1, MIER2 and MIER3 would be most likely to mediate the interaction. Sequence alignment of the three isoforms reveals three regions with moderate conservation (Figure 2E). Deletion of either region 1 or 2, but not 3, resulted in failure of MIER1 to co-purify with the H2A:H2B heterodimer (Figure 3D–G, Supplementary Figure S1b). Since regions 1 and

2 contain many negatively charged residues, it is important to rule out a non-specific interaction with the positively charged histone dimer. Therefore, to confirm that this interaction is specific we made MIER1 amino-terminal constructs in which the order of amino acids in regions 1 or 2 was scrambled. In both cases, MIER1 no longer co-purifies with the H2A:H2B dimer confirming a stereo-specific interaction (Figure 3H, I).

To obtain a structural model of the interaction of MIER1(aa:17–75) regions 1 and 2 with H2A:H2B, we used Alphafold2 multimer to predict the mode of binding (Figure 4A–C, Supplementary Figure S2). The resulting model is structurally convincing and reveals how the MIER1 sequence has complementary stereochemistry to the H2A:H2B dimer surface. Overall the interface area between MIER1 and the histone dimer is 2005 $Å^2$ (27). Region 1 is predicted with high confidence and adopts an extended configuration interacting with H2B through a conserved phenylalanine interacting in a non-polar pocket with residues Y43, I55 and M60 in H2B. Region 2 is also predicted with high confidence, to form a helix making numerous non-polar interactions with the other end of H2B. Between regions 1 and 2 there are three additional helices containing many negatively charged residues that interact with the positively charged surface of the H2A:H2B dimer that interacts with DNA in the assembled nucleosome. Importantly, Alphafold2 multimer predictions in which region 3 was included, suggested that region 3 plays no role in the interaction with the H2A:H2B histone dimer. To support the Alphafold model we designed mutations in regions 1 and 2 (Figure 4c and Supplementary Figure S3). As expected, mutations S71A/L72A did not disrupt the complex since they are oriented away from the histone dimer. Mutations I66A/L69A/L70A in region 2 essentially abolished interaction as expected since they make multiple interactions with the histone dimer. Mutations F22A/M28A/L29A in region 1 were not sufficient to disrupt the complex. This is surprising given that scrambling or deletion of region 1 did abolish interaction. Potentially the non-polar alanine mutations allow some residual interaction of this region and the other interactions are sufficient to maintain interaction.

The MIER proteins can bind to H2A:H2B in the context of a histone octamer, but not when assembled into a nucleosome

As mentioned above, we noticed that the MIER proteins sometimes co-purify not only with H2A and H2B, but also with histones H3 and H4 (Figure 2D). This suggests that the MIER proteins can bind to H2A:H2B in the context of a full histone octamer. Given that H3:H4 are always lost during gel filtration, we suggest that this is a relatively weak, indirect interaction mediated by H2A:H2B binding. Interestingly, the Alphafold2 model of MIER1 regions 1 and 2 (aa:17–75) bound to the H2A:H2B dimer appears to partially occlude the surface of H2B that interacts with histone H4 in the H3:H4 tetramer (Figure 4B and F).

To explore this further, we expressed MIER1(aa:1–177) with a GST-tag in bacterial cells. This protein is significantly proteolyzed during purification from bacteria, consistent with being an intrinsically disordered protein. However, the degraded mixture is clearly able to pull-down a histone oc-

tamer, albeit with some dissociation of H3:H4, likely due to reduced stability of the octamer in low-salt buffer (Figure 4D). In contrast, no histone octamer binding was observed for the GST-only control (Figure 4D).

Given that we experimentally observed that the MIER1 amino-terminal region is able to bind to a histone octamer, we generated a further Alphafold2 multimer model including MIER1(aa:17–75) together with eight histone proteins. In this model MIER1 binds to the H2A:H2B dimer in the octamer context, exactly as the isolated H2A:H2B dimer, with the exception that the helix corresponding to the conserved region 2 is displaced and now interacts with histone H4. Figure 4F shows the Alphafold2 model in the context of a full histone octamer compared with the DNA-wrapped nucleosome (Figure 4G). Importantly, neither GST-MIER1(aa:1–177), nor the GST-only control were able to interact with an intact DNA-wrapped nucleosome (Figure 4E).

The BAH domain from BAHD1 interacts with the MIER1:HDAC1 complex and recruits endogenous C1QBP

The Bromo-Adjacent-Homology-Domain containing protein 1 (BAHD1) has been identified as being a core component of the MIER1:HDAC1 complex (13,14). BAHD1 consists of a carboxy-terminal BAH domain with an intrinsically disordered amino-terminal region containing a proline-rich region (Figure 5A). We co-expressed the BAH domain from BAHD1(aa:525–780) together with the MIER1:HDAC1 complex confirming that the BAH domain is sufficient for interaction with the MIER1:HDAC1 complex (Figure 5B).

Interestingly in these purifications we consistently observed an additional band with a molecular weight of around 28 kDa that co-purifies with a fraction of the complex. MS analysis of this gel band identified it as the protein C1QBP (aka: ASF/SF2-associated protein p32) (Supplementary Table S1). This 282 aa protein is known to undergo a maturation process that removes a mitochondrial targeting sequence (aa:1–73) from the amino terminus leaving a mature protein of around 23 kDa. To confirm the identity of this protein we performed a western blot with an antibody against the full-length protein. Figure 5C clearly shows that C1QBP is present in the lysate (lane 1) and strongly enriched in the purified complex (lane 2). To confirm the specificity of the antibody, we expressed a full-length C1QBP protein with an amino-terminal HA-tag that blocks maturation of the protein. This has an expected molecular weight of 33 kDa (Figure 5C, lanes 3 and 4). From this, it seems that the co-purified version of C1QBP is the mature form, consistent with the MS data (Supplementary Table S1) which did not identify any peptides from the amino-terminal 73 amino acids.

The MIER1:HDAC1:BAHD1:C1QBP complex specifically recruits intact nucleosomes bearing H3K27me2/3 marks

Analysis of the gel filtration fractions following MIER1:HDAC1:BAHD1-BAH:C1QBP purification, shows that the earlier fractions contain all four histones H2A, H2B, H3 and H4 (Figure 5B). In contrast later
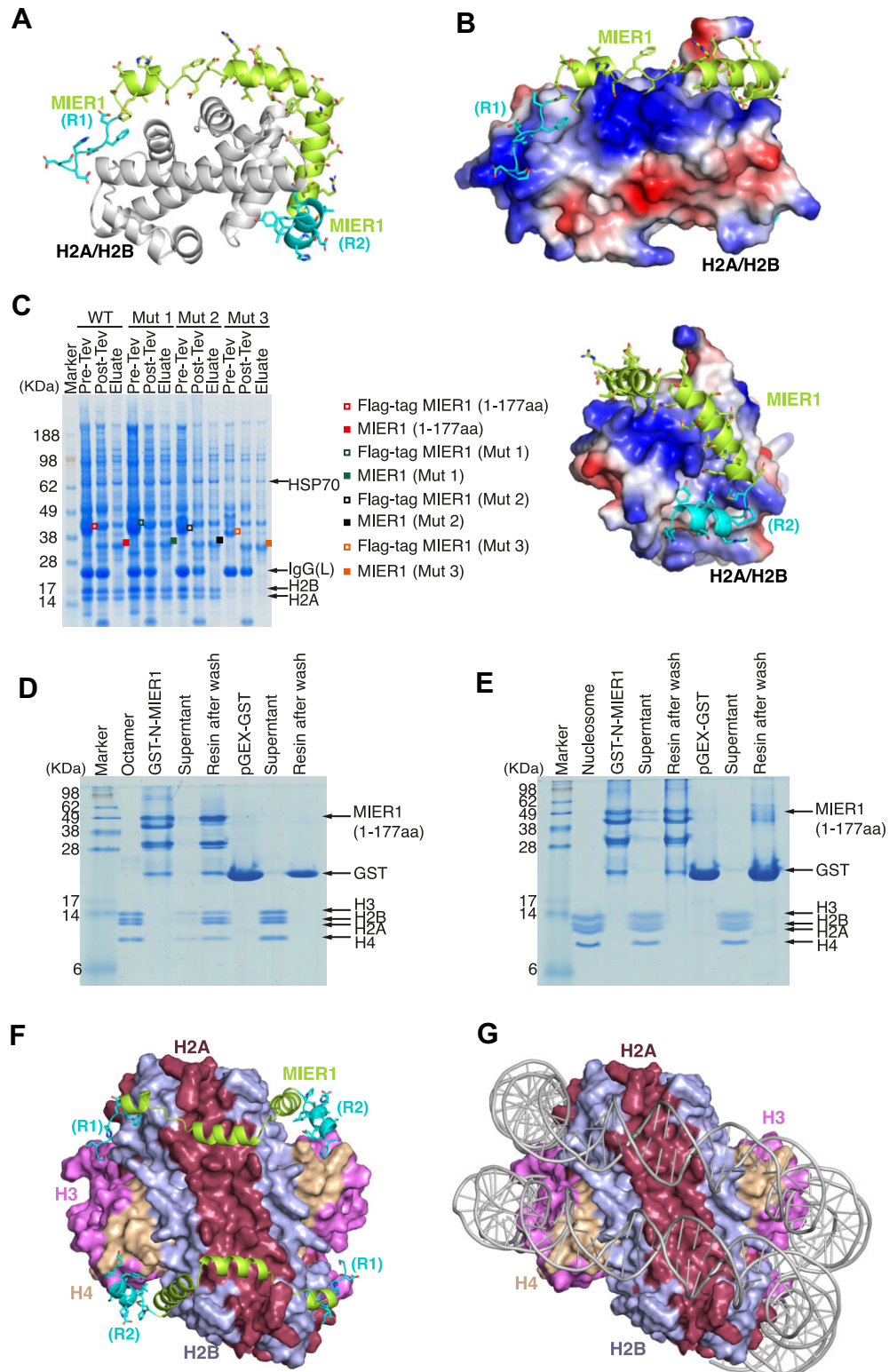
Figure 4. The amino-terminal region of MIER1(aa:1–177) binds a full histone octamer. (**A**) Alphafold2 model of the interaction of MIER1(aa:17–75) (lime green/cyan) with an H2A:H2B dimer (grey cartoon). (**B**) Alphafold2 model of the the interaction of MIER1(aa:17–75) (lime green/cyan) binding to H2A:H2B (electrostatic surface) and the model rotated 260° clockwise about y-axis. (**C**) The FLAG tagged amino-terminus of wild type MIER1(aa:1–177) (red symbols), Mutation 1 (S71A, L72A) (green symbols), Mutation 2 (F22A, M28A, L29A) (purple symbols) purified with histone H2A:H2B dimer, the Mutation 3 (I66A, L69A, L70A) (orange symbols) does not bind to histones (sequences shown in Supplement Figure S3). (**D**) GST pull down experiments confirm the ability of the amino-terminus of MIER1(aa:1–177) to bind a full histone octamer. (**E**) GST pull down experiments show that the amino-terminus of MIER1(aa:1–177) does not bind to a DNA-wrapped nucleosome. (**F**, **G**) Comparison of the Alphafold2 model for the binding of the amino-terminal region of MIER1(aa:17–75) to a histone octamer with a DNA-bound nucleosome.
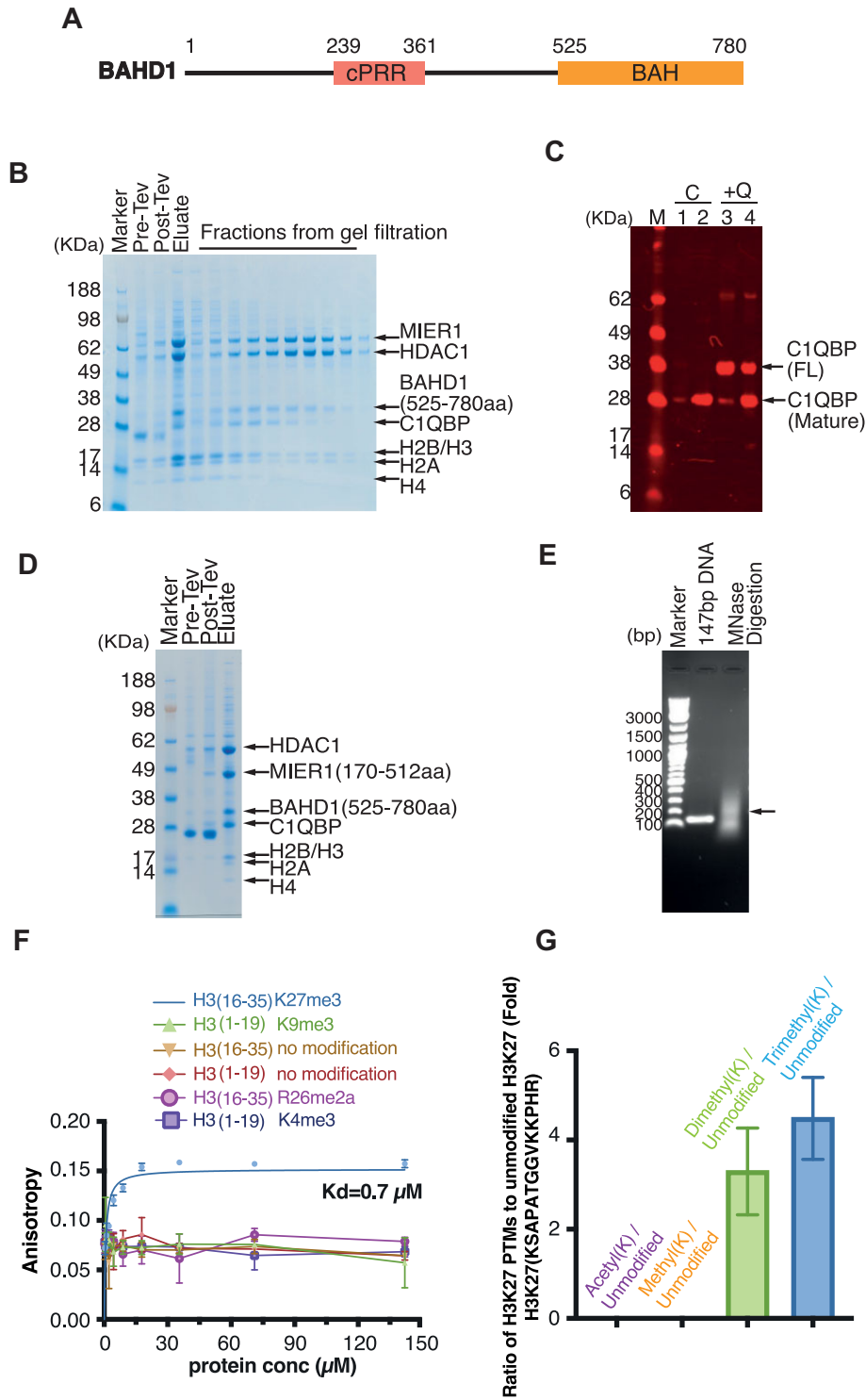
Figure 5. The MIER1:HDAC1:BAHD1 complex forms a stoichiometric complex with endogenous C1QBP and a nucleosome. (**A**) Schematic of the domain structure of full-length BAHD1. (**B**) The FLAG-tagged MIER1(aa:1–512):HDAC1: BAHD1(aa:525–780) complex was purified using anti-FLAG resin and a Superdex S200 column. The endogenous C1QBP and H2A:H2B:H3:H4 co-purified with the whole complex. (**C**) Lanes 1 (lysate) and 2 (anti-FLAG purified) are from a co-transfection of MIER1(aa:171–512):HDAC1:BAHD1(aa:525–780) (labelled C). Lanes 3 (lysate) and 4 (anti-FLAG purified) are from a co-transfection of MIER1(aa:171–512):HDAC1:BAHD1(aa:525–780) with the addition of C1QBP (labelled + Q). The western blot was visualized using mouse anti-C1QBP antibody followed by goat anti-mouse 680RD. (**D**) Co-purification of the MIER1(aa:171–512): HDAC1:BAHD1(aa:525–780) complex to show that the H2A:H2B:H3:H4 co-purified with MIER1 lacking the amino-terminus. (**E**) Purified DNA obtained by micrococcal nuclease digestion of the purified MIER1(aa:171–512):HDAC1:BAHD1(aa:525–780):C1QBP:Nucleosome complex analysed in a 1× TBE 1% agarose gel. (**F**) Fluorescence anisotropy assay of the binding of the various modified histone peptides to the BAH domain of BAHD1. Error bars indicate ± s.e.m. (*n* = 3). (**G**) Quantitative MS analysis of histones that co-purified with the MIER1(aa:171–512):HDAC1: BAHD1:C1QBP complex reveals that the majority of H3K27 is di or tri-methylated.

fractions contain only H2A:H2B. We initially hypothesised that a full histone octamer was binding to the amino-terminal region of MIER1 and that the presence of BAHD1:C1QBP might partly stabilise histone octamer binding so that it survives size exclusion chromatography. However, the histones appear to be supra-stoichiometric suggestive that the complex may have pulled down polynucleosomes, which would not be the expected behaviour for the amino-terminal region of MIER1.

To explore this further we co-expressed MIER1(aa:171–512) lacking the amino-terminal region with HDAC1 and BAHD1. In this experiment the MIER1 still co-purified with all four histones (Figure 5D). This supports the concept that the BAH domain from BAHD1 (or perhaps the co-purified C1QBP) is able to recruit nucleosomes. To confirm this, we asked whether or not the histones that we co-purified in this complex are assembled with nucleic acid. We treated the peak fraction with micrococcal nuclease and analysed the released DNA on an agarose gel. We observed a smear between 100 and 250 bp which is consistent with nucleosomal DNA (Figure 5E).

It has previously been shown that the BAH domain from BAHD1 recognises H3 histone tails bearing a K27me3 modification (10). We confirmed this interaction using a fluorescence anisotropy assay (Figure 5F). We also used MS analysis to quantify the post-translational modifications on the histones that co-purified with the MIER1(aa:171–512):HDAC1:BAHD1-BAH:C1QBP complex (Supplementary Table S2). Importantly we found that the vast majority of histone H3 that co-purifies with the complex carries either di- and tri-methylation on H3K27, consistent with specific recognition by the BAH domain (Figure 5G). Interestingly no acetylated lysine residues were detectable, consistent with efficient deacetylation by HDAC1 in the complex.

DISCUSSION

The MIER proteins recruit the deacetylase enzymes, HDAC1/2, via a conserved ELM2-SANT domain in the same way that the MIDEAS, MTA and RCOR proteins assemble the MiDAC, NuRD and CoREST complexes (5–7). Unlike the multimeric MiDAC and NuRD complexes, the MIER1 complex is monomeric (5,7).

The finding that the MIER1 amino-terminal region has H2A:H2B/histone octamer binding activity suggests that the complex may potentially play a role as a histone chaperone. This, in turn, suggests that the complex may be involved in either depositing or removing histones from chromatin. The Alphafold2 model of the MIER1 amino-terminal region bound to an H2A:H2B dimer makes excellent stereochemical sense, giving confidence that it is likely to be accurate. Importantly, the model also has numerous features in common with other peptide chaperones that bind H2A:H2B. Like ANP32E, Swr1, YL1, Chz1 and APLF, MIER1 has numerous acidic residues that interact with the DNA-binding surface of H2A:H2B (28–32). The MIER1 region (aa:17–75) overlaps closely with the other chaperones (except Chz1) which all have an aromatic residue (Y/F/W) that interacts with a non-polar pocket in the histone dimer (Supplementary Figure S4).

MIER1(aa:17–75) follows a trajectory round the histone dimer similar to YL1 and Chz1 although the details of the interactions are different (33). Interestingly the model of the interaction of MIER1 with H2A:H2B has the largest solvent-excluded surface of all these chaperone complexes, consistent with the finding that the complex co-purifies over several columns.

The experimental finding that MIER1 can bind to a complete histone octamer fits with the Alphafold2 model, but requires a reorientation of the region 2 alpha helix to avoid occluding the surface of the H2B that interacts with histone H4. This reorientation was seen in the Alphafold2 model of MIER1 bound to a complete octamer. Experimental structural biology would be required to confirm these models. The ability of a peptide to act as a chaperone for an intact histone octamer has only been observed once before, for the APLF peptide (32,34). The MIER1:octamer complex would appear to allow initial binding of DNA to the H3:H4 dyad position. We presume the DNA could then wrap around the octamer in both directions displacing the MIER1 complex.

The histone-binding activity of MIER1 is unexpected and it appears that, of the six known HDAC1/2 complexes, only the MIER complex has this activity. Importantly, this activity is common to all three MIER proteins. Indeed, MIER homologues in D. melanogaster (Uniprot A1Z6Z7) and C. elegans (Uniprot P91437) show 47% and 37% identity compared with MIER1, respectively, in the amino-terminal region that we have shown interacts with the H2A:H2B histone dimer (Supplementary Figure S5). This suggests that histone-binding activity is conserved. Interestingly, MIER1 knockout mice are viable, albeit with metabolic dysfunction (13). It may of course be that MIER2 and MIER3 are able to compensate for the loss of MIER1 in these animals and that mice lacking all three genes would not be viable.

Genome-targeted HDAC complexes typically contain domains or sequence motifs, or accessory proteins that mediate interaction with chromatin (35). The MIER complex has been reported to associate with the chromodomain protein CDYL and the BAH domain protein BAHD1 (10,13,36). When we co-expressed MIER1 with HDAC1 and the BAH domain from BAHD1 we found that the endogenous protein C1QBP co-purified with the complex in apparently stoichiometric amounts. This association of C1QBP with the MIER1 complex is unexpected and raises questions as to its role. C1QBP is an enigmatic, multi-functional protein present in multiple cellular compartments (37). It has an amino-terminal 73 residue mitochondrial-targeting sequence that is cleaved during maturation (38). The carboxy-terminal 208 residues form a trimeric ring, doughnut-like structure (39). It has been reported to have roles in the regulation of apoptosis, pre-mRNA-splicing, mitochondrial protein synthesis and to act as a receptor for C1q at the cell membrane (40,41). Perhaps more relevant for the MIER complex, C1QBP has also been reported to have a role in transcriptional regulation and homologous recombination (42). A recent report suggests that, intriguingly, C1QBP can act as a chaperone of histones H3 and H4 (43). This is supported by proteomic studies which identify that C1QBP interacts with all four
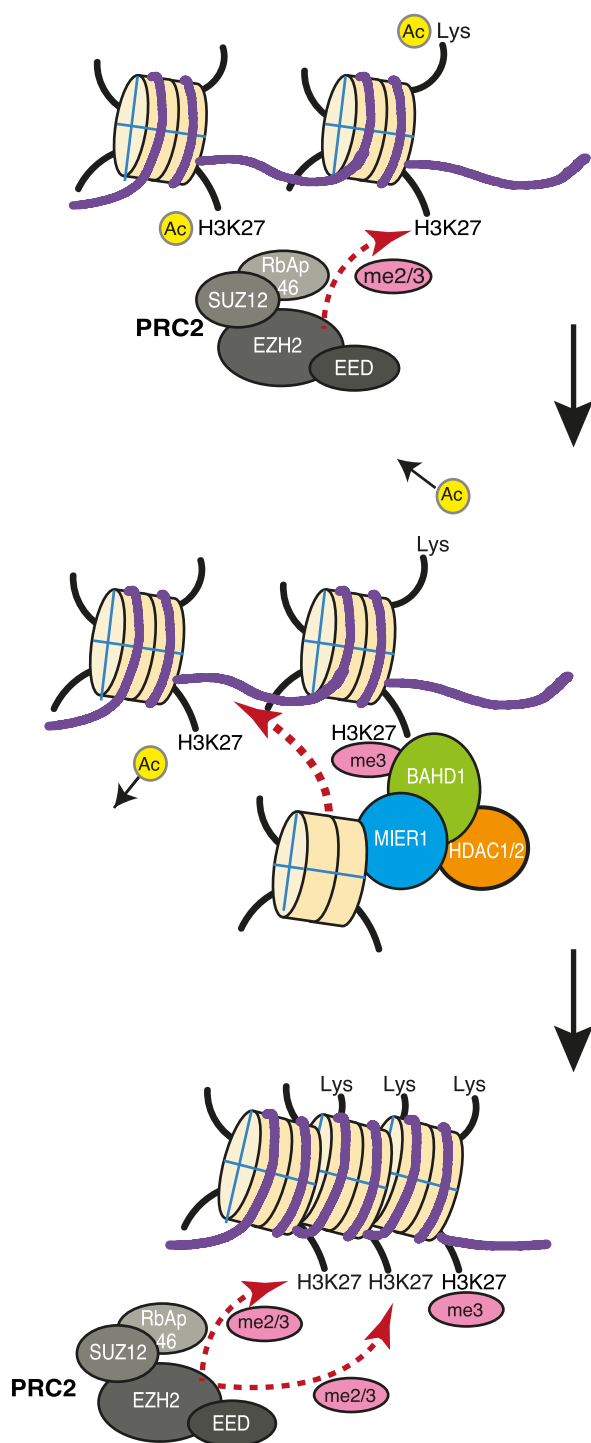
Figure 6. Proposed collaboration between the MIER1 and PRC2 complexes. PRC2 adds di-and tri- methyl marks to H3K27 to induce transcriptional repression. The MIER1 complex is recruited to chromatin through interaction with the H3K27me2/3 marks recognized by the BAH domain in BAHD1. This results in histone deacetylation and deposition of histone octamer feeding forward to enable the PRC2 complex to add further H3K27me2/3 marks.

core histones and, interestingly, four proteins in the PRC2 repression complex (44,45).

Both this study and previous studies by others, suggest that the MIER1 complex is recruited to chromatin via in-

teraction of the BAHD1-BAH domain with H3K27me3 marks (10). These marks are deposited by the PRC2 repressor complex leading to heterochromatin formation and gene repression. Interestingly, MIER1 has also been reported to form a complex with CDYL (13,36), another reader of H3K27me2/3 marks. The finding that a deacetylase complex is recruited to this mark, suggests a feedforward mechanism through which HDAC1/2 removes proximal H3K27ac marks, and perhaps other Kac marks such as H3K9ac (46), shutting down transcription and facilitating further methylation by PRC2. Since acetyl-lysine marks are associated with promoters and enhancers that typically have reduced nucleosome occupancy, it is tempting to speculate that the histone-binding activity of the MIER complex allows it to act as a chaperone to deposit histone octamer at these sites thereby increasing nucleosome density and contributing to the formation of heterochromatin (Figure 6).

The intriguing observation of the juxtaposition of a deacetylase enzyme together with a potential histone octamer chaperone and H3K27me2/3 nucleosome-binding activity is both unexpected and unprecedented, but would fit well with a role for the MIER complex in shutting down active transcription.

DATA AVAILABILITY

Raw MS data and searched results from MaxQuant are available from PRIDE (https://www.ebi.ac.uk/pride/) with identifier PXD040685.

SUPPLEMENTARY DATA

Supplementary Data are available at NAR Online.

ACKNOWLEDGEMENTS

FUNDING

REFERENCES

1. Seto,E. and Yoshida,M. (2014) Erasers of histone acetylation: the histone deacetylase enzymes. *Cold Spring Harb. Perspect. Biol.*, **6**, a018713.

2. Wang,L., Charroux,B., Kerridge,S. and Tsai,C.C. (2008) Atrophin recruits HDAC1/2 and G9a to modify histone H3K9 and to determine cell fates. *EMBO Rep.*, **9**, 555–562.

3. Clark,M.D., Marcum,R., Graveline,R., Chan,C.W., Xie,T., Chen,Z., Ding,Y., Zhang,Y., Mondragon,A., David,G. *et al.* (2015) Structural insights into the assembly of the histone deacetylase-associated Sin3L/Rpd3L corepressor complex. *Proc. Natl. Acad. Sci. U.S.A.*, **112**, E3669–E3678.

4. Derwish,R., Paterno,G.D. and Gillespie,L.L. (2017) Differential HDAC1 and 2 recruitment by members of the MIER family. *PLoS One*, **12**, e0169338.

5. Turnbull,R.E., Fairall,L., Saleh,A., Kelsall,E., Morris,K.L., Ragan,T.J., Savva,C.G., Chandru,A., Millard,C.J., Makarova,O.V. *et al.* (2020) The MiDAC histone deacetylase complex is essential for embryonic development and has a unique multivalent structure. *Nat. Commun.*, **11**, 3252.

6. Song,Y., Dagil,L., Fairall,L., Robertson,N., Wu,M., Ragan,T.J., Savva,C.G., Saleh,A., Morone,N., Kunze,M.B.A. *et al.* (2020) Mechanism of crosstalk between the LSD1 demethylase and HDAC1 deacetylase in the CoREST complex. *Cell Rep.*, **30**, 2699–2711.

7. Millard,C.J., Fairall,L., Ragan,T.J., Savva,C.G. and Schwabe,J.W.R. (2020) The topology of chromatin-binding domains in the NuRD deacetylase complex. *Nucleic Acids Res.*, **48**, 12972–12982.

8. Hendrich,B., Guy,J., Ramsahoye,B., Wilson,V.A. and Bird,A. (2001) Closely related proteins MBD2 and MBD3 play distinctive but interacting roles in mouse development. *Genes Dev.*, **15**, 710–723.

9. Cowley,S.M., Iritani,B.M., Mendrysa,S.M., Xu,T., Cheng,P.F., Yada,J., Liggitt,H.D. and Eisenman,R.N. (2005) The mSin3A chromatin-modifying complex is essential for embryogenesis and T-cell development. *Mol. Cell. Biol.*, **25**, 6990–7004.

10. Fan,H., Guo,Y., Tsai,Y.H., Storey,A.J., Kim,A., Gong,W., Edmondson,R.D., Mackintosh,S.G., Li,H., Byrum,S.D. *et al.* (2021) A conserved BAH module within mammalian BAHD1 connects H3K27me3 to Polycomb gene silencing. *Nucleic Acids Res.*, **49**, 4441–4455.

11. Blackmore,T.M., Mercer,C.F., Paterno,G.D. and Gillespie,L.L. (2008) The transcriptional cofactor MIER1-beta negatively regulates histone acetyltransferase activity of the CREB-binding protein. *BMC Res. Notes*, **1**, 68.

12. Paterno,G.D., Li,Y., Luchman,H.A., Ryan,P.J. and Gillespie,L.L. (1997) cDNA cloning of a novel, developmentally regulated immediate early gene activated by fibroblast growth factor and encoding a nuclear protein. *J. Biol. Chem.*, **272**, 25591–25595.

13. Lakisic,G., Lebreton,A., Pourpre,R., Wendling,O., Libertini,E., Radford,E.J., Le Guillou,M., Champy,M.F., Wattenhofer-Donze,M., Soubigou,G. *et al.* (2016) Role of the BAHD1 chromatin-repressive complex in placental development and regulation of steroid metabolism. *PLoS Genet.*, **12**, e1005898.

14. Huttlin,E.L., Bruckner,R.J., Paulo,J.A., Cannon,J.R., Ting,L., Baltier,K., Colby,G., Gebreab,F., Gygi,M.P., Parzen,H. *et al.* (2017) Architecture of the human interactome defines protein communities and disease networks. *Nature*, **545**, 505–509.

15. Callebaut,I., Courvalin,J.C. and Mornon,J.P. (1999) The BAH (bromo-adjacent homology) domain: a link between DNA methylation, replication and transcriptional regulation. *FEBS Lett.*, **446**, 189–193.

16. Bierne,H., Tham,T.N., Batsche,E., Dumay,A., Leguillou,M., Kerneis-Golsteyn,S., Regnault,B., Seeler,J.S., Muchardt,C., Feunteun,J. *et al.* (2009) Human BAHD1 promotes heterochromatic gene silencing. *Proc. Natl. Acad. Sci. U.S.A.*, **106**, 13826–13831.

17. Armache,K.J., Garlick,J.D., Canzio,D., Narlikar,G.J. and Kingston,R.E. (2011) Structural basis of silencing: sir3 BAH domain in complex with a nucleosome at 3.0 A resolution. *Science*, **334**, 977–982.

18. Kuo,A.J., Song,J., Cheung,P., Ishibe-Murakami,S., Yamazoe,S., Chen,J.K., Patel,D.J. and Gozani,O. (2012) The BAH domain of ORC1 links H4K20me2 to DNA replication licensing and Meier-Gorlin syndrome. *Nature*, **484**, 115–119.

19. Patel,D.J. (2016) A structural perspective on readout of epigenetic histone and DNA methylation marks. *Cold Spring Harb. Perspect. Biol.*, **8**, a018754.

20. De Ioannes,P., Leon,V.A., Kuang,Z., Wang,M., Boeke,J.D., Hochwagen,A. and Armache,K.J. (2019) Structure and function of the Orc1 BAH-nucleosome complex. *Nat. Commun.*, **10**, 2894.

21. Fan,H., Lu,J., Guo,Y., Li,D., Zhang,Z.M., Tsai,Y.H., Pi,W.C., Ahn,J.H., Gong,W., Xiang,Y. *et al.* (2020) BAHCC1 binds H3K27me3 via a conserved BAH module to mediate gene silencing and oncogenesis. *Nat. Genet.*, **52**, 1384–1396.

22. Lowary,P.T. and Widom,J. (1998) New DNA sequence rules for high affinity binding to histone octamer and sequence-directed nucleosome positioning. *J. Mol. Biol.*, **276**, 19–42.

23. Garcia,B.A., Mollah,S., Ueberheide,B.M., Busby,S.A., Muratore,T.L., Shabanowitz,J. and Hunt,D.F. (2007) Chemical derivatization of histones for facilitated analysis by mass spectrometry. *Nat. Protoc.*, **2**, 933–938.

24. Sidoli,S., Kori,Y., Lopes,M., Yuan,Z.F., Kim,H.J., Kulej,K., Janssen,K.A., Agosto,L.M., Cunha,J., Andrews,A.J. *et al.* (2019) One minute analysis of 200 histone posttranslational modifications by direct injection mass spectrometry. *Genome Res.*, **29**, 978–987.

25. Cox,J. and Mann,M. (2008) MaxQuant enables high peptide identification rates, individualized p.p.b.-range mass accuracies and proteome-wide protein quantification. *Nat. Biotechnol.*, **26**, 1367–1372.

26. Evans,R., O'Neill,M., Pritzel,A., Antropova,N., Senior,A., Green,T., Žídek,A., Bates,R., Blackwell,S., Yim,J. *et al.* (2021) Protein complex prediction with AlphaFold-Multimer. bioRxiv doi: https://doi.org/10.1101/2021.10.04.463034, 10 March 2022, preprint: not peer reviewed.

27. Krissinel,E. and Henrick,K. (2007) Inference of macromolecular assemblies from crystalline state. *J. Mol. Biol.*, **372**, 774–797.

28. Zhou,Z., Feng,H., Hansen,D.F., Kato,H., Luk,E., Freedberg,D.I., Kay,L.E., Wu,C. and Bai,Y. (2008) NMR structure of chaperone Chz1 complexed with histones H2A.Z-H2B. *Nat. Struct. Mol. Biol.*, **15**, 868–869.

29. Obri,A., Ouararhni,K., Papin,C., Diebold,M.L., Padmanabhan,K., Marek,M., Stoll,I., Roy,L., Reilly,P.T., Mak,T.W. *et al.* (2014) ANP32E is a histone chaperone that removes H2A.Z from chromatin. *Nature*, **505**, 648–653.

30. Hong,J., Feng,H., Wang,F., Ranjan,A., Chen,J., Jiang,J., Ghirlando,R., Xiao,T.S., Wu,C. and Bai,Y. (2014) The catalytic subunit of the SWR1 remodeler is a histone chaperone for the H2A.Z-H2B dimer. *Mol. Cell*, **53**, 498–505.

31. Latrick,C.M., Marek,M., Ouararhni,K., Papin,C., Stoll,I., Ignatyeva,M., Obri,A., Ennifar,E., Dimitrov,S., Romier,C. *et al.* (2016) Molecular basis and specificity of H2A.Z-H2B recognition and deposition by the histone chaperone YL1. *Nat. Struct. Mol. Biol.*, **23**, 309–316.

32. Corbeski,I., Dolinar,K., Wienk,H., Boelens,R. and van Ingen,H. (2018) DNA repair factor APLF acts as a H2A-H2B histone chaperone through binding its DNA interaction surface. *Nucleic Acids Res.*, **46**, 7138–7152.

33. Huang,Y., Dai,Y. and Zhou,Z. (2020) Mechanistic and structural insights into histone H2A-H2B chaperone in chromatin regulation. *Biochem. J.*, **477**, 3367–3386.

34. Corbeski,I., Guo,X., Eckhardt,B.V., Fasci,D., Wiegant,W., Graewert,M.A., Vreeken,K., Wienk,H., Svergun,D.I., Heck,A.J.R., van Attikum,H., Boelens,R. *et al.* (2022) Chaperoning of the histone octamer by the acidic domain of DNA repair factor APLF. *Sci. Adv.*, **8**, eabo0517.

35. Millard,C.J., Watson,P.J., Fairall,L. and Schwabe,J.W.R. (2017) Targeting class I histone deacetylases in a "complex" environment. *Trends Pharmacol. Sci.*, **38**, 363–377.

36. Bantscheff,M., Hopf,C., Savitski,M.M., Dittmann,A., Grandi,P., Michon,A.M., Schlegl,J., Abraham,Y., Becher,I., Bergamini,G. *et al.* (2011) Chemoproteomics profiling of HDAC inhibitors reveals selective targeting of HDAC complexes. *Nat. Biotechnol.*, **29**, 255–265.

37. Sengupta,A., Banerjee,B., Tyagi,R.K. and Datta,K. (2005) Golgi localization and dynamics of hyaluronan binding protein 1 (HABP1/p32/C1QBP) during the cell cycle. *Cell Res.*, **15**, 183–186.

38. Ghebrehiwet,B., Lim,B.L., Peerschke,E.I., Willis,A.C. and Reid,K.B. (1994) Isolation, cDNA cloning, and overexpression of a 33-kD cell surface glycoprotein that binds to the globular "heads" of C1q. *J. Exp. Med.*, **179**, 1809–1821.

39. Jiang,J., Zhang,Y., Krainer,A.R. and Xu,R.M. (1999) Crystal structure of human p32, a doughnut-shaped acidic mitochondrial matrix protein. *Proc. Natl. Acad. Sci. U.S.A.*, **96**, 3572–3577.

40. Peterson,K.L., Zhang,W., Lu,P.D., Keilbaugh,S.A., Peerschke,E.I. and Ghebrehiwet,B. (1997) The C1q-binding cell membrane proteins cC1q-R and gC1q-R are released from activated cells: subcellular distribution and immunochemical characterization. *Clin. Immunol. Immunopathol.*, **84**, 17–26.

41. Petersen-Mahrt,S.K., Estmer,C., Ohrmalm,C., Matthews,D.A., Russell,W.C. and Akusjarvi,G. (1999) The splicing factor-associated protein, p32, regulates RNA splicing by inhibiting ASF/SF2 RNA binding and phosphorylation. *EMBO J.*, **18**, 1014–1024.

42. Matsumoto,K., Kose,S., Kuwahara,I., Yoshimura,M., Imamoto,N. and Yoshida,M. (2018) Y-box protein-associated acidic protein (YBAP1/C1QBP) affects the localization and cytoplasmic functions of YB-1. *Sci. Rep.*, **8**, 6198.

43. Lin,J., Bao,X. and Li,X.D. (2021) A tri-functional amino acid enables mapping of binding sites for posttranslational-modification-mediated protein-protein interactions. *Mol. Cell*, **81**, 2669–2681.

44. Oliviero,G., Brien,G.L., Waston,A., Streubel,G., Jerman,E., Andrews,D., Doyle,B., Munawar,N., Wynne,K., Crean,J. *et al.* (2016) Dynamic protein interactions of the polycomb repressive complex 2 during differentiation of pluripotent cells. *Mol. Cell. Proteomics*, **15**, 3450–3460.

45. Zhang,X., Zhang,F., Guo,L., Wang,Y., Zhang,P., Wang,R., Zhang,N. and Chen,R. (2013) Interactome analysis reveals that C1QBP (complement component 1, q subcomponent binding protein) is associated with cancer cell chemotaxis and metastasis. *Mol. Cell. Proteomics*, **12**, 3199–3209.

46. Wang,Z.A., Millard,C.J., Lin,C.L., Gurnett,J.E., Wu,M., Lee,K., Fairall,L., Schwabe,J.W. and Cole,P.A. (2020) Diverse nucleosome site-selectivity among histone deacetylase complexes. *Elife*, **9**, e57663 .